The very early-age behaviour of Ultra-High Performance Concrete containing ground granulated blast furnace slag

Soufien Moula, Amor Ben Fraj, Thomas Wattez, Marwen Bouasker, Nizar Bel Hadj Ali

The very early-age behaviour of Ultra-high performance concrete containing ground granulated blast furnace slag

Soufien Moula [a,b,c], Amor Ben Fraj[a], Thomas Wattez[d], Marwen Bouasker[b], Nizar Bel Hadj Ali[e]

[a] Cerema, Univ Gustave Eiffel, UMR MCD, F-77171, Sourdun, France

[b] Université d'Orléans, INSA Centre Val de Loire, Université de Tours, Laboratoire de Mécanique Gabriel Lamé Polytech Orléans, 8 rue Léonard de Vinci, 45072 Orléans, France

[c] Laboratoire de Génie Civil, Ecole Nationale d'Ingénieurs de Tunis, Université de Tunis El Manar, B.P. 37, Le Belvédère 1002, Tunis, Tunisia

[d] Ecocem Materials Ltd, 4 place Louis Armand, 75012 Paris, FRANCE

[e] Modelling in Civil Engineering and Environment, National Engineering School of Gabes, University of Gabes, Gabes 6029, Tunisia

A B S T R A C T

Ultra-high performance concrete (UHPC), despite being a relatively new kind of advanced cement-based material (featuring outstanding mechanical performance and excellent durability), has been deemed unsustainable due to its high cement content, thus increasing its carbon footprint. The large amounts of cement and silica fume (SF) can also raise both production costs and cracking risks due to the high early-age autogenous shrinkage. This paper addresses an innovative approach for developing a more sustainable UHPC involving an efficient application of ground granulated blast furnace slag (GGBS). Slags of two fineness levels are used, displaying a Blaine fineness of 420 m²/kg (SL1) and 700 m²/kg (SL2), respectively. These slags have been incorporated as volume replacements for 30% and 50% cement.

The results analysis shows that it is indeed possible to produce SL2-based UHPC with a behavior similar to that of classical silica fume-based materials. The partial replacement of ordinary Portland cement (OPC) by 30% of GGBS (SL1 or SL2) improves workability, promotes the hydration reaction of cement and accelerates setting. In this case, the nucleation site effect of GGBS particles dominates; it seems to be directly correlated with the fineness of the slag used. Thus, the finer additions result in a significant acceleration of setting and hydration. The dilution effect is more sensitive at 50% of SL1 substitution. This prevailing effect delays the hydration reaction, prolongs setting times and decreases the peak of heat flow. In contrast however, this delay effect was not observed for the mixture containing 50% of SL2. Shrinkage measurements indicated that 30% of SL1 induces a slight reduction in early-age chemical and autogenous types of shrinkage. The most severe shrinkage is clearly found in mixtures incorporating 30% of SL2. This phenomenon may be due to the distribution of refined pores, which increases capillary tension. A more sustainable UHPC containing a high level of superfine slag (50%) with less autogenous shrinkage has been successfully produced.

Keywords: UHPC, GGBS, Fineness, Hydration, Chemical shrinkage, Autogenous shrinkage

1. Introduction

Ultra-high performance concrete (UHPC) or, using a more specific term, ultra-high performance fiber reinforced concrete (UHPFRC) is an emerging cement-based composite with excellent mechanical properties and durability, exceeding those of conventional concrete [1]. It is, however, worth mentioning that the high cement content (800-1,200 kg/m^3) significantly expands the carbon footprint of concrete elements, raises manufacturing costs and releases more heat of hydration [2]. The cement industry is responsible for about 7% of global CO_2 emissions [3,4]. With the world tending towards a greener type

of construction practices, one of the key sustainability challenges over the few next decades will be to design and produce concrete with less clinker and capable of inducing lower CO_2 emissions than conventional concrete, while offering the same reliability and even better durability [5,6]. Consequently, several studies have shown that replacing cement by supplementary cementitious materials (SCM) proves to be the most widely practiced approach to reducing the CO_2 footprint of cementitious materials [7]. It has been documented that considerable amounts of cement can be replaced in UHPC without significantly impairing the material's compressive strength [6]. SCMs, such as SF, fly ash (FA) [8], rice husk ash (RHA) [9] and blast furnace slag (BFS), can all be used to satisfy numerous technical performance requirements, in addition to sustainability performance criteria for low-emission concrete development. To reduce the cement content in UHPC, GGBS is commonly used to substitute a portion of the cement [7, 10-16].

GGBS has been used as an SCM in concrete for many years. As is not the case with most SCMs, it has been established that GGBS possesses both hydraulic and pozzolanic properties [8]. Due to its hydraulic behavior, GGBS reacts with water and generates C-S-H [17], which in turn allows the concrete to retain adequate strength and durability even after a large amount of cement has been substituted by GGBS [7]. According to the literature, the properties of UHPC evolve rapidly at an early age. Generally speaking, the early-age behavior of this advanced concrete can be described by the following parameters: workability, hydration kinetics, setting time, chemical and autogenous shrinkage, and strength development [18]. UHPC has been designed and investigated with the aim of decreasing the amount of Portland cement while maintaining high performance and good workability in the fresh state. UHPC is a super-plasticized concrete renowned for its satisfactory fluidity [19]. It was found that GGBS improves the overall workability of concretes and enhances their durability [20]. For example, the authors reported that by replacing silica fume with fine BFS, the slump flow was increased by 70 mm. Abdulkareem *et al.* [11] reported that replacing 30% of cement with slag induced a decrease in SP content (58%), as required to achieve the mini slump flow of the reference mixture. Moreover, they explained this effect by an improved packing density, since the slag fineness lies between that of cement and that of SF, as well as by the particles' cohesion and viscosity. The results of the study conducted by Luzu *et al.* [21] revealed that both the mineralogical properties and the fineness of the additions play a decisive role in the saturation dosage and SP impact on packing density. The hydration process of cementitious ingredients in UHPC is similar to that in conventional concrete under standard curing conditions [14]. However, the phase development in UHPC is expected to be kinetically and quantitatively different from that in ordinary concretes. In addition, it is expected that heat flow and microstructure will be largely affected by integrating pozzolanic additives [22]. GGBS is chemically activated by $Ca(OH)_2$ and gypsum in cement, but its rate of hydration is lower than that of clinker [23], which slows strength development at the early age of UHPC. Pyo and Kim [20] confirmed that GGBS slows the hydration process and increases setting time, which impairs early mechanical properties. Moreover, the use of high-range water reducing admixtures can hinder the hydration reaction, which in turn prolongs setting time and reduces early-age mechanical strength [2].

In order to use massive quantities of slag, it is recommended to incorporate a moderate level of silica fume (SF). Even though SF guarantees advanced properties, many authors have varying opinions regarding the definition of an optimal content that enables achieving the greatest strength. According to previous studies [24], the optimal level replacement lies around 25% of Portland cement. SF, initially considered as an industrial waste, has become a relatively expensive component in formulating concrete products, and its demand has been consistently rising [25]. Therefore, it is critical to expand the types and sources of SCMs for developing sustainable UHPC with less SF content. GGBS can generate additional C–S–H upon hydration while decelerating early strength gain when no activator is present in the system [23]. Some strategies adopted have sought to prevent the low reactivity of slag, such as

chemical activation by alkalis and thermal activation at a specific high temperature and for a specific duration [15]. Also, one way to accelerate the hydration and strength development in UHPC incorporating slag consists in modifying its fineness. It was found that GGBS of a varying fineness provides a different surface area for the hydration reaction and moreover influences the distribution of hydration products in the cement matrix, which can impact the strength and durability of UHPC [17]. It is worth noting that research works using high fineness slag in multi-component UHPC are indeed very scarce [17].

Due to the presence of a large fraction of superfine particles and the extremely low water-to-binder ratio of UHPC (w/b = 0.15-0.25), the risk of high shrinkage has to be considered [26]. If such a large shrinkage occurs, this will lead to residual tension, which in turn may induce the formation of cracks and further degrade the durability of UHPC, thereby rapidly reducing the service life of engineering structures [27]. At a very early age, the fresh UHPC mixture presents a potential risk of cracking, as a result of the more pronounced shrinkage, whether chemical or autogenous in origin. The former stems from chemical volume contraction during the hydration process while the latter is induced by the self-desiccation of cement-based material. Chemical shrinkage develops during cement hydration because of the smaller absolute volume of the hydration products than that of the reactants [28]. It should be pointed out that research works carried out on the chemical shrinkage of multi-component UHPC systems are very limited. Li *et al.* [29] evaluated the chemical shrinkage of UHPC pastes with different types and dosages of superplasticizer (SP). They found that various types of SP exert more of an effect on the chemical shrinkage development rate before 24 h; afterwards, they remain nearly the same. Zenati *et al.* [30] highlighted the influence of the BFS of EL-Hadjar on the chemical shrinkage of UHPC at a very early age (i.e. before 72 h). Their experimental results showed that chemical shrinkage of the reference mixture was greater because UHPC contains significant amounts of clinker minerals. However, BFS-based UHPCs display a lower shrinkage; this shrinkage is even lower with a higher BFS content. Thus, the fundamental early-age material properties of UHPC need to be quantified precisely in order to control the premature shrinkage cracks for practical application.

Autogenous shrinkage is defined as the apparent volume reduction of a mixture containing cementitious materials during their hydration. It results from the internal consumption of moisture [28]. It has been documented that both the chemical and autogenous types of shrinkage of UHPC are particularly high at the early age, due to the use of low w/b, a high content of fine cementitious materials and the absence of coarse aggregates [29,31,32]. According to previous studies, it has been found that SCMs are indeed able to modify pore structure through chemical and physical effects; this modification is closely related to autogenous shrinkage [33]. Each addition exhibits distinctly different effects on pore structure, due to their varying physical properties and activities. It has been documented that the impact of slag on UHPC shrinkage might possibly depend on the type of slag [34]. The incorporation of high-level slag can accelerate the water consumption rate while reducing the critical radius of capillary pores, hence increasing autogenous shrinkage development. This phenomenon explains why some investigations have reported a pronounced autogenous shrinkage of UHPC when slag was added [35]. Ghafari *et al.* [36] conducted an experimental work aimed at substituting SF by other fine SCMs, such as GGBS and FA, in order to reduce the amount of autogenous shrinkage, yet without altering concrete mechanical properties. Liu *et al.* [37] proved that the inclusion of GGBS can increase autogenous shrinkage. These authors highlighted that the pozzolanic reaction of GGBS increases the consumption of calcium hydroxide, which in turn increases water consumption. More generally, the incorporation of slag increases the autogenous shrinkage of the cement matrix [38]. Lee *et al.* [39] concluded that all GGBS-based concretes exhibited greater autogenous shrinkage than conventional concretes with the same w/b ratio. They attributed this finding to the higher chemical shrinkage induced by the incorporation of GGBS, which led to faster and greater self-desiccation, thus resulting in more severe autogenous

shrinkage. At the same time, the pore structure of the GGBS-containing samples was observed to be finer than that of the reference specimen. This finer pore structure gives rise to a larger incidence of capillary stress, promoting self-desiccation and raising the autogenous deformation [40]. However, due to the different experimental conditions and the variety of mineral additions used, the conclusions regarding the effect of GGBS on the autogenous shrinkage of cementitious materials were, once again, inconsistent and even contradictory. Although many studies on cement-based materials have been conducted, the effects of GGBS on autogenous shrinkage are still unclear. It is worth noting that the vast majority of research works have focused on measuring the linear autogenous shrinkage of UHPC after 24 hours of hydration. However, very few studies have been dedicated to very early-age autogenous shrinkage. Motivated by the scarcity of test data on the early-age behavior of UHPCs, in particular autogenous shrinkage, the objective of this comprehensive experimental work is to study the effect of replacing cement with slag on autogenous deformations from the first few minutes after mixing.

The aforementioned literature review shows that, despite the considerable body of works published in the literature on UHPC prepared with all kinds of SCMs (which are promising substitutes for cement in UHPC production), few studies have in effect examined the coupled effect of slag replacement and slag fineness on the early-age properties of standard-cured UHPC. The main objective of this paper is to design an eco-friendly UHPC incorporating GGBS, as a volume cement replacement at a low SF content, without the activation of slag by additional chemicals or thermal treatments. To better quantify the influence of GGBS content and fineness on the early-age behavior of UHPC, a characterization of the workability, reaction rate measurements, setting time, chemical shrinkage and volumetric autogenous shrinkage has been performed on eight UHPC pastes prepared with the same water-to-cementitious materials ratio (w/b = 0.16) and various dosages of OPC, GGBS and SP.

2. Experimental methodology

2.1. Materials

In this study, UHPC mixtures are designed to satisfy both fresh and hardened state requirements. Ordinary Portland Cement (OPC, CEM I 52.5 N), produced by Holcim (Le Teil plant), was used. The main characteristics of this type of cement are a high amount of silica and a low C_3A content. **Figure 1** shows the XRD patterns of cement with identification of the main current phases (C_3S, C_2S, C_3A and C_4AF). The mineralogical composition of the cement using the Bogue calculation is listed in **Table 1**. The supplementary cementitious materials (SCMs) included both silica fume (SF) provided by Condensil and slag of two different levels of fineness (ordinary slag SL1 and superfine slag SL2) from Ecocem, as a partial replacement of the cement in UHPC systems. The XRD patterns of these materials are depicted in **Figure 2**. The XRD analysis indicates that these materials are almost exclusively amorphous. The vitreous nature of the slag is clearly demonstrated by a large halo on the XRD pattern. The fine peaks observed are due to the presence of some crystallized phases, however they are practically negligible. The chemical compositions of the cementitious materials, as determined by X-ray fluorescence (XRF) analysis, and their main physical properties are given in **Table 1**.

Quartz Sand (QS, CV32) with a median diameter (d50) of 248 µm, supplied by Sibelco, was used as the fine aggregate. The SiO_2 content of this QS is about 98.78%. Its Blaine fineness and density are 124 cm^2/g and 2.65, respectively. Crushed Quartz (CQ, C500), also sold by Sibelco, was used as a partial substitution of SF. Its median diameter (d50) was approx. 6 µm. Its Blaine specific surface area and density are 10,435 cm^2/g and 2.65, respectively; it is a totally crystallized material (99.61% of SiO_2).

A high-range water reducer polycarboxylate Sika Viscocrete Krono-20 HE superplasticizer (SP) was selected to adjust the fresh properties of UHPC. Its density and solid content are 1.085 and 41%, respectively; this additive was introduced to ensure the self-compactness of the produced UHPC.

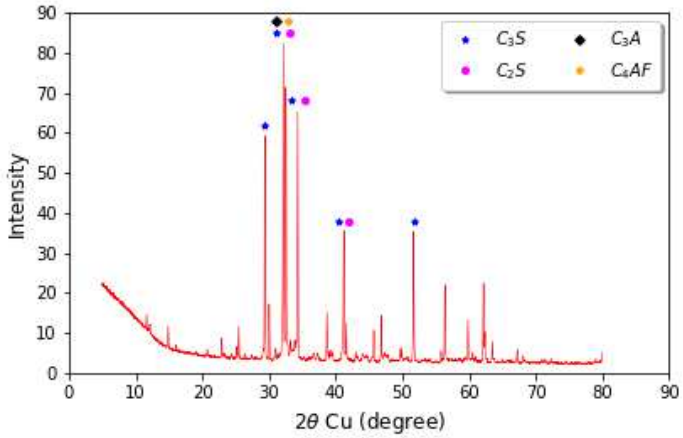

Figure 1 : *XRD patterns of used cement.*

Table 1
Chemical composition and physical properties of different components.

Components' identification	Component	Cement	Silica Fume	Ordinary Blast-Furnace-Slag	Superfine Blast-Furnace Slag
	Trade name	CEM I 52.5 N	S95 B DM	–	–
	Plant	Le Teil	Condensil	Ecocem	Ecocem
	Abbreviation	C/OPC	SF	SL1	SL2
Chemical composition (% mass)	CaO	63.93	0.34	42.34	44.04
	SiO_2	27.67	98.63	36.61	36.72
	Al_2O_3	3.00	0.17	11.19	10.08
	Fe_2O_3	2.27	0.06	0.44	0.43
	K_2O	0.09	0.24	0.42	0.46
	MgO	0.73	0.22	7.50	7.96
	Na_2O	0.10	0.01	0.36	0.28
	SO_3	1.70	0.06	1.56	0.51
	MnO	0.08	0.01	0.16	0.15
	TiO_2	0.14	0.00	0.72	0.66
	P_2O_5	0.06	0.01	0.00	0.01
	SrO	0.15	0.00	0.07	0.09
	LOI	1.71	0.91	0.83	0.32
Physical properties	Blaine specific area (cm^2/g)	3630	–	4200	7000
	BET specific area (m^2/g)	–	25	–	–
	Density (-)	3.17	2.24	2.90	2.90
	d(50) (µm)	–	–	11.00	5.00
Mineralogical composition (%)	C_3S	67.00			
	C_2S	17.00			
	C_3A	4.00			
	C_4AF	7.00			

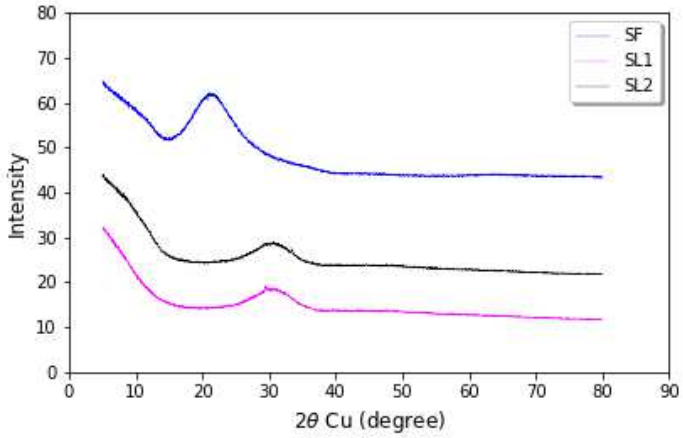

Figure 2 : *XRD patterns of used SCM (SF, SL1, SL2 and SL3).*

2.2. Mix proportions and mixing

The UHPC mix design was originally formulated by Richard and Cheyrezy [24]. This relatively new cementitious composite was further improved to account for material availability [11,41] and allow for optimization in this study, with the requisite reduction in SF content. The aim of using silica fume in low quantities is to reduce production costs, reduce the carbon footprint and to be able to incorporate massive quantities of slag given the high pozzolanic activity of silica fume. A reference mix design (Ref_{SF}), integrating 1,025 kg/m^3 of cement, was proposed. The cement was partially substituted by 12% (valued by mass) of both SF and CQ. Three-quarters of this replacement rate was for SF while the other quarter was for CQ. GGBS with two different levels of fineness (SL1 and SL2) was used in order to further refine the design of our UHPC. To balance the differences in total absolute volumes, due to the various densities of cementitious materials (OPC, GGBS and SF), two levels of GGBS volume percentages were explored (30% and 50%). The mix volume was maintained constant. GGBS was incorporated to produce more sustainable UHPC mixes. This study also addresses the possibility of producing a UHPC without SF. Thus, a second reference formula (Ref_{SL2}), based on superfine slag (SL2), was also investigated. A volume substitution of SF by superfine slag was initiated. From this basic mixture of UHPC, two mixes containing 30% of SL1 and SL2, as a volume cement replacement, were designed. The removal of silica fume is intended to further reduce cost and carbon footprint of UHPC. The water-to-binder (w/b) ratio was maintained at 0.16 for all analyzed mixes. QS, CQ and water contents were all held constant. The superplasticizer dosage was adjusted to achieve the same concrete workability; this workability was evaluated through mini slump flow tests and targeted 35 cm for UHPC. It should be noted that the total water amount refers to the sum of water in the superplasticizer and the water added to the solution (SP + water). The eight UHPC compositions, as defined above, are detailed in **Table 2**.

Table 2
Mix proportions of UHPCs.

Proportions of used materials for one cubic meter (kg/m^3)										
Mix name	Mix code	OPC	QS	SF	CQ	SL1	SL2	SP	SP (%)	W
Reference (SF)	Ref_{SF}	1025.00	1127.50	92.25	30.75	-	-	32.45	2.20	151.23
30% SL1 (SF)	SL1-30$_{SF}$	717.50	1127.50	92.25	30.75	281.31	-	20.65	1.40	163.03
50% SL1 (SF)	SL1-50$_{SF}$	512.50	1127.50	92.25	30.75	468.85	-	35.40	2.40	148.28
30% SL2 (SF)	SL2-30$_{SF}$	717.50	1127.50	92.25	30.75	-	281.31	11.80	0.80	171.88
50% SL2 (SF)	SL2-50$_{SF}$	512.50	1127.50	92.25	30.75	-	468.85	17.70	1.20	165.98
Reference (SL2)	Ref_{SL2}	1025.00	1127.50	-	30.75	-	119.43	29.50	2.00	154.18
30% SL1 (SL2)	SL1-30$_{SL2}$	717.50	1127.50	-	30.75	281.31	119.43	17.70	1.20	165.98

30% SL2 (SL2)	$SL2\text{-}30_{SL2}$	717.50	1127.50	-	30.75	-	400.74	14.75	1.00	168.93

In order to ensure the self-compacting function, all selected UHPC mixtures were prepared in a 15-L intensive mixer (Eirich). This high-energy mixer, as shown in **Figure 3**, features a star-blade, inclined drum and high mixing speed (opposing currents). First, the dry constituents (sand, cement and SCMs) were mixed for 30 s at low speed. Next, the solution containing the water and SP was added to the container. Mixing continued at high speed for 4 min. The mixing protocol mentioned above resulted in an optimal dispersion of particles and a high mixture homogenization with a reduced mixing time. At the end of mixing, a flowable UHPC mix was obtained. Although it is known that elephant skin formation can be observed on the surface of UHPC, which typically contains extremely high superplasticizer amount, seconds to minutes after casting [42,43], this phenomenon can be considered as negligible in our study as all the selected mixes were optimized so that the mixture does not exhibit any bleeding or segregation.

After completing these mixing processes, the fresh UHPC sample was transferred to the container within 5 min in order to examine the early-age properties of the designed mixes (flow table test, isothermal calorimetry measurements, setting time, chemical and autogenous shrinkage).

Figure 3 : *Eirich mixer used.*

2.3. Testing methods

2.3.1. Slump flow

Once mixing was completed, mini slump flow tests of the various fresh UHPC mixes were conducted according to EN 12350-8 [44]; the average of two measurements of the sample spread was recorded. The targeted spread value of the investigated UHPC mixes was set at around 350 ± 20 mm, as supported by the analysis of previous findings [11], so as to achieve a sufficient release of entrapped air and satisfactory strength performance.

2.3.2. Isothermal calorimetry

A multi-channel isothermal calorimeter (model TAM Air, TA Instruments) was used to measure the heat flow and cumulative heat of hydration of all considered mixtures. Each measurement was performed continuously at a constant temperature of 20°C during the first 7 days of hydration. Immediately after mixing, approximately 15 g of fresh material were placed into a 20-mL plastic ampoule, accurately weighed (± 0.001 g) and stored in the measurement channels. The first measurement was acquired about 10 min after the initial contact between binder and mixing water. The curves provided in this paper are average curves computed from the test results obtained on two parallel specimens.

2.3.3. *Vicat setting time*

The initial and final setting times of UHPC mixtures were determined by an automatic Vicat set-up (with a measurement interval of 10 min) in accordance with the standard specification EN 196-3 [45]. For each UHPC sample, two Vicat tests were carried out to determine the average setting time. This study considers that the initial setting time corresponds to the elapsed time, as measured from zero until the time at which the distance between the needle and the base-plate reaches 5 mm (between 3 and 6 mm according to the European Standard [45]). However, as a result of UHPC shrinkage (due to the very low w/b), final setting time corresponded to 5 mm of penetration for all mixes and not 0.5 mm, as specified by the standard.

2.3.4. *Chemical shrinkage*

Measurements were recorded on the various UHPC mixes by ensuring the permanent water saturation of the hydrating cement matrix pore space. The hydrostatic weighing method used in the present investigation allows, with the simple experimental system diagrammed in **Figure 4**, recording automatic and continuous measurements of Le Chatelier's contraction [46,47]. The gravimetric technique consists in monitoring the variation in buoyancy of a sample of cementitious material placed in a flask with an orifice on its cap. Immediately after mixing, 15-20 g of fresh sample are introduced into a 20-ml cylindrical flask. Entrapped air bubbles are removed at a roughly 1-min vibration sequence. The remaining empty flask volume is then carefully filled with distilled water, while avoiding any perturbation of the specimen. The contact surface between the top of the sample and the exterior water equals about 4 cm². Afterwards, the entire system, including the sample in its flask, is hung on a scale (accuracy: ± 0.0001 g) by a nylon thread and immersed in distilled water. Data acquisition starts 10 min after the initial contact between binder and mixing water. The test system is placed in an air-conditioned room at 20° ± 1°C. The quasi-isothermal conditions during the experiment are assured by a peripheral water circulation system under a cryostat-controlled temperature.

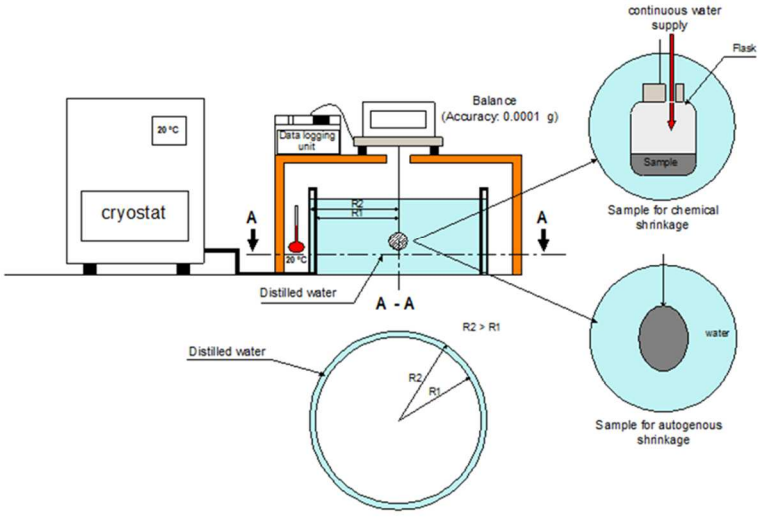

Figure 4 : *Schematic of the test device used for chemical and autogenous shrinkage measurement.*

2.3.5. *Autogenous shrinkage*

The same device for measuring chemical shrinkage is also used to monitor the early-age volumetric autogenous shrinkage of all selected mixtures. At the end of mixing, about 80-120 g of fresh cementitious material are introduced into a latex membrane. Before closing the elastic rubber, the

greatest level of care must be taken to guarantee that air is being discharged. The excess membrane is then cut off and the sample is cleaned and weighed. Next, the test specimen is placed on a nacelle hung from a balance and immediately immersed in the water bath. The balance is connected to a computer for automatic and continuous recording of system buoyancy variations. The measurement of volume change starts 15 min after water-binder contact. Some researchers have used this measurement in a dynamic configuration to evaluate the volumetric deformation of cementitious matrices with high w/c ratios, which consequently are highly sensitive to bleeding [48]. In this study, an identical w/b (0.16) has been used for all UHPC mixtures. At this lower ratio, the matrix packing density is optimal and the mixture does not present any bleeding or segregation. For this reason, the measurement under a static configuration has been adopted.

The volumetric deformations are converted into linear deformations ($\varepsilon_{vol\rightarrow lin}$) by means of Equation [1]:

$$\varepsilon_{vol\rightarrow lin}(t) = \frac{10^6}{3} \times \frac{\Delta M\,(t)}{V\,(t_0)\times \rho}\,[1]$$

where: $\varepsilon_{vol\rightarrow lin}(t)$ is the autogenous shrinkage (µm/m), $\Delta M\,(t)$ the mass variation of the sample under water (g) at time t, ρ the density of water at 20°C (0.9982 g/cm^3), and $V\,(t_0)$ the initial volume of the sample (cm^3).

3. Results and interpretation

3.1. Workability

The workability of the designed UHPC should be carefully managed to ensure their onsite properties. This key parameter was measured herein in terms of flow diameter so as to estimate the necessary superplasticizer content for blended-cement UHPC, thus yielding the same workability as the reference material. To reach the same spread value (350 ± 20 mm), the SP dosage was adjusted. The required SP dosages to achieve a 35-cm slump flow for all selected UHPC mixtures are given in **Figure 5**.

The optimal SP dosages of the reference concretes (Ref_{SF} and Ref_{SL2}) are 2.2% and 2.0%, respectively. The SP content of the reference formula Ref_{SL2} is slightly lower than that of the reference mix Ref_{SF}. This lower SP content is justified by the ability of superfine granulated furnace slag (SL2) to improve workability of the mix. Such a positive effect can be partly attributed to the smooth and dense surface characteristics of the slag particles producing the slip planes [37]. The fineness of SF is significantly higher than that of SL2. It is known that SF particles increase water demand, with this effect often being directly ascribed to their extremely high specific surface area [49]. The amount of SP required to disperse SF particles depends on the specific surface area of SF. The addition of SF particles is clearly correlated with a higher SP content required to recover similar workability. These results are in agreement with those of Pyo and Kim [20], who found that the partial substitution of SF by slag resulted in a 70-mm improvement in slump flow.

It can be seen from **Figure 5** that the 30% substitution of cement by SL1 ($SL1\text{-}30_{SF}$) and SL2 ($SL2\text{-}30_{SF}$) induces a drop in the SP content required to achieve the mini slump flow of Ref_{SF} (by relative amounts of -36.4% and -63.6%, respectively). A reduction in SP dosage is also observed for SL2-based mixtures instead of SF. The SP dosage decreased from 2% (Ref_{SL2}) to 1.2% and 1% for $SL1\text{-}30_{SL2}$ and $SL2\text{-}30_{SL2}$, respectively. These results underscored a considerable improvement in UHPC flowability when low levels of slag are incorporated into the mix. The addition of GGBS to the mixes had a significant effect on the water amount required to achieve better workability. Two phenomena, occurring simultaneously, serve to explain the decrease in SP dosage: i) the drop in the quantity of C_3A reduces early AFt formation, which eventually enhances mix workability [50]; and ii) the enhancement of

packing first and then particle cohesion and viscosity [11]. Slag can increase the packing density of UHPC due to its fine volume, which can fill voids among the coarser cementitious particles. Introducing GGBS makes the mixture more cohesive and decreases bleeding water and segregation, which ultimately enhances the rheological behavior of concrete in the fresh state. The results obtained are consistent with those of Kim *et al.* [51], who measured, for the same SP content, an improvement in slump flow by 9% and 16% when slag content was respectively 15% and 30%. The incorporation of SL2 yields better homogeneity and packing. Since packing and workability are closely correlated, the inclusion of such small particles in a cementitious mix is expected to enhance the particle packing density, which is typically coupled with improved rheological properties [11,52]. For SL1-50$_{SF}$ and despite the increase in the amount of GGBS, the required SP content to reach the mini slump flow of the reference concrete equals 2.4%. The lubrication effect of GGBS along with the fluidizing effect of superplasticizer seem to be mitigated by the water demand of GGBS particles. At a high replacement rate, SL1 can absorb some of the free mixing water and SP due to its high specific surface area, which decreased particle dispersion. A large amount of water in the mix was absorbed by SL1 particles, which ultimately led to a decrease in workability (increased SP content). As a result, water available for lubrication remains insufficient, allowing for the free movement of particles [53]. However, a lower amount of SP (1.2%) is needed to disperse the superfine particles of the SL2-50$_{SF}$ mixture. This decline confirms the beneficial effect of a high fineness slag. Thanks to their filling effect, SL2 particles enhance matrix packing and promote cohesion, which in turn improves the rheological properties of UHPC. The beneficial effect of SL2 is attributed to the superfine particles that both fill the spaces created by larger OPC particles and reduce the frictional forces of a dual OPC-SL2 material, resulting in high fluidity of the OPC-SL2 system. This effect is also tied to the decrease in the amount of C_3A, due to the decrease in cement content, which also induces improved workability.

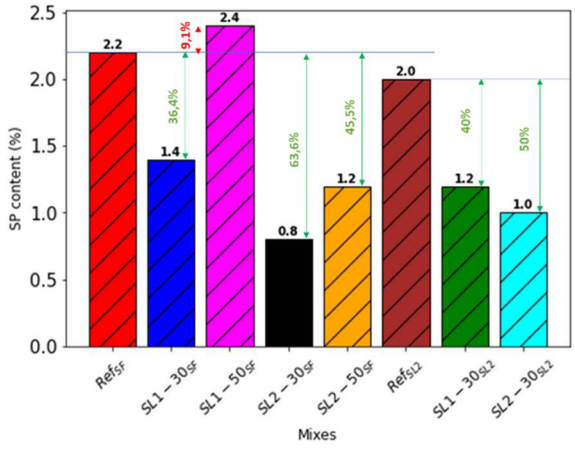

Figure 5 : *Required SP dosages.*

3.2. Heat of hydration

In order to better understand the influence of the different levels of fineness and contents of GGBS on the early-age reactivity of UHPC pastes, isothermal calorimetry tests were conducted at 20°C over the first 7 days. Heat flows and the cumulative heat release, normalized per gram of binder, are presented in **Figures 6** and **7**, respectively. **Table 3** summarizes the primary measured characteristic values of the isothermal hydration curves.

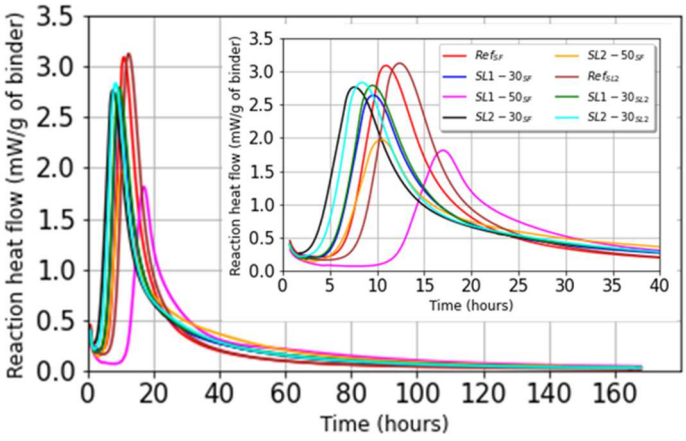

Figure 6 : *Hydration heat flow of investigated UHPC mixtures.*

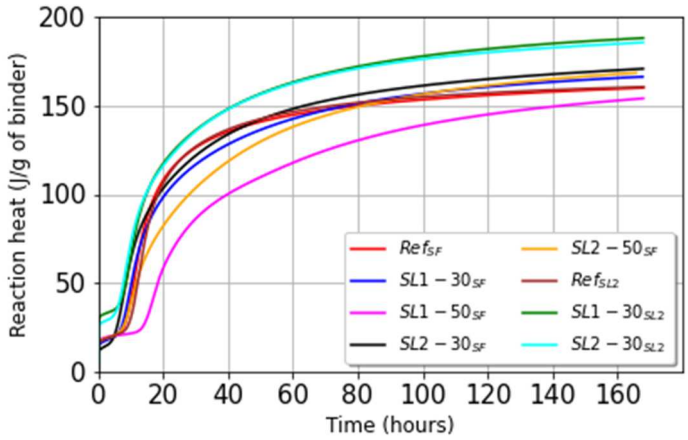

Figure 7 : *Cumulative heat of investigated UHPC mixtures.*

Table 3
Peaks of hydration of UHPC mixes.

Samples	Cumulated heat of reaction		Time of maximum heat flow t_{max}		Maximum intensity of heat flow	
	Measured value Q_{max} (J/g binder)	Normalized value $\frac{Q_{max}}{Q_{max}(Ref)}$ (−)	Measured value t_{max} (min)	Normalized value $\frac{t_{max}}{t_{max}(Ref)}$ (−)	Measured value I_{max} (mW/g binder)	Normalized value $\frac{I_{max}}{I_{max}(Ref)}$ (−)
Ref_{SF}	160	1	657	1	3.1	1
$SL1\text{-}30_{SF}$	166.2	1.04	576	0.88	2.6	0.84
$SL1\text{-}50_{SF}$	153.9	0.96	1019	1.55	1.8	0.58
$SL2\text{-}30_{SF}$	170.7	1.07	455	0.69	2.8	0.90
$SL2\text{-}50_{SF}$	168.5	1.05	626	0.95	2	0.65
Ref_{SL2}	160.5	1	744	1.13	3.1	1
$SL1\text{-}30_{SL2}$	188.1	1.18	572	0.87	2.8	0.90
$SL2\text{-}30_{SL2}$	185.5	1.16	506	0.77	2.8	0.90

The following section will discuss the influence of GGBS dosage and fineness on the UHPC hydration process. As expected, the replacement of clinker by GGBS up to 50% without changing w/b ratio does affect the hydration reaction.

For reference mixtures Ref_{SF} and Ref_{SL2}, it is apparent that the influence of SF and SL2 on the early hydration kinetics of the developed UHPC is very similar, which can be demonstrated by the relatively small difference between their respective times to reach the maximum hydration peak. As observed, these two reference mixtures exhibit the same heat flow peak, i.e. approximately 3.1 mW/g of binder.

The time to reach the maximum reaction heat flow is 657 min for Ref_{SF}, while this peak appears after 744 min for Ref_{SL2}. This phenomenon can be attributed to the ability of SF to accelerate the hydration rate of UHPC by means of nucleation and the growth site effect [54]. The presence of extremely fine SF particles promotes the nucleation effect by acting as additional nucleation sites for hydrates, which in turn results in rapid hydration [55]. Recently, Yalçınkaya and Çopuroˇglu [14] measured a heat flow of about 3 mW/g of binder for a UHPC manufactured with 881 kg/m^3 of cement and 176 kg/m^3 of SF, based on the calorimetry test results. The peak of heat flow curves at 20°C was reached at 636 min. These findings are in accordance with results obtained in this study. **Figure 7** shows that both Ref_{SF} and Ref_{SL2} display the same profile of hydration characteristics. The maximum heat reaction for Ref_{SF} and Ref_{SL2} are respectively 160 and 160.5 J/g of binder. During the early stages, the SF-based mix exhibited high activity and accelerated the hydration rate, as compared to SL2. In 2022, Xi *et al.* [56] conducted an experimental study on the effect of SF on UHPC hydration and strength development. Their isothermal calorimetry test results revealed that SF accelerates cement hydration intensively at an early age. An important point to note is that even though the SP dosage for the Ref_{SF} mixture slightly exceeds that of the Ref_{SL2} mixture, an accelerating effect of SF is observed compared to SL2. This phenomenon is mainly attributed to the physical effect of SF particles.

Slag replacement reduced the magnitude of heat flow, while total heat released during the first 7 days was not proportional to the GGBS replacement ratio, thus indicating that slag participated in the exothermic reaction of the binder hydration [57]. An increase in the dosage of both SL1 and SL2 significantly decreased the peak reaction heat flow value. Compared to the Ref_{SF} and Ref_{SL2} mixtures, it appears that a 30% volume substitution of cement by GGBS (SL1-30_{SF}, SL2-30_{SF}, SL1-30_{SL2} and SL2-30_{SL2}) produces nearly the same heat flow peak, i.e. about 2.6-2.8 mW/g of binder. As presented in **Table 3**, the heat flow peaks of these various concrete mixes occur at 576, 455, 572 and 506 min for SL1-30_{SF}, SL2-30_{SF}, SL1-30_{SL2} and SL2-30_{SL2}, respectively. Therefore, slag fineness does not exert a considerable effect on the peak value, but mainly on the time corresponding to the heat flow peak in these systems. The influence of low GGBS content on UHPC hydration seems rather small, and the profile of hydration characteristics of these four mixtures exhibits practically the same behavior, with a slight difference in the time to reach the maximum reaction heat flow. As shown in **Figure 7**, the maximum heat reactions for SL1-30_{SF}, SL2-30_{SF}, SL1-30_{SL2} and SL2-30_{SL2} are 166.2, 170.7, 188.1 and 185.5 J/g of binder, respectively. In the presence of SL2 and SF particles (SL2-30_{SF}), the heat flow peak occurs at 202 and 121 min before that of Ref_{SF} and SL1-30_{SF}, respectively. When SF is replaced by SL2 (SL2-30_{SL2}), the heat flow peak appears 238 and 66 min before that of Ref_{SL2} and SL1-30_{SL2}, respectively. It can therefore be concluded that at low replacement levels, SL1 and SL2 accelerate the hydration process through their nucleation effect. Another explanation for this acceleration effect lies in the reduced SP content in mixtures that incorporate a low slag content.

Slag fineness can serve as an activator for the hydration of cementitious matrix materials. Consequently, an increase in slag fineness accelerates UHPC hydration due to the relatively high reactivity of superfine particles. The hydration of slag occurs when enough $Ca(OH)_2$ is being produced by cement and slag (hydraulic part) hydration and/or when the alkalinity of the pore solution is sufficiently high (pH > 11) [57]. SL2 can react more quickly than SL1 and generate more C-S-H gel more quickly as well. Therefore, the activity of SL2 should be much higher than that of SL1 in UHPC at an early age. Slag is chemically activated by the $Ca(OH)_2$ and gypsum in cement, but its reaction speed is slow, whereas SF reacts with $Ca(OH)_2$ first in UHPC because of its high fineness [37]. For the mixes containing 30% of GGBS, the early stage of hydration was accelerated; this finding can be attributed to a reduction in the amount of SP. It was observed that increasing slag fineness leads to a reduction in SP content, with this effect being directly correlated with the physical effect of finely granulated blast furnace slag.

Figure 6 shows that with an increase in the slag replacement rate, the peak value of the exothermic reaction decreases significantly. The maximum heat reaction and heat flow peak of SL1-50_{SF} equal respectively 153.9 J/g of binder and 1.8 mW/g of binder; moreover, the time to reach the maximum reaction heat flow is 1,019 min. For this mixture, the dilution effect dominates the nucleation effect. Increasing slag fineness leads to an increase in both the heat flow peak and reaction heat being released. For SL2-50_{SF} concrete, the maximum heat reaction and heat flow peak are respectively 168.5 J/g of binder and 2 mW/g of binder. The time to achieve the maximum reaction heat flow is reduced by 393 min (626 vs. 1,019 min). This acceleration can be attributed to the lower SP content, i.e. 1.2% vs. 2.2% for the Ref_{SF} mixture and 2.4% for the SL1-50_{SF} concrete. Some authors have characterized the retardation effect of SP as follows: the inclusion of SP prevents solid phase nucleation and hydration products from growing, thus resulting in a delay in cement hydration [58]. The lower hydraulic activity of GGBS is mainly related to its potential to dissolve and react in generating subsequent hydrated products. This phenomenon depends on slag rate: the higher the GGBS dosage, the greater the dilution effect. Consequently, the reaction heat decreases, which in turn decelerates the hydration reaction [11].

This study suggests that the presence of a low content of GGBS results in a reduction of SP content, which can largely accelerate the cement hydration process. This paper has shown that an elevated level of high fineness slag (50% of SL2) has an accelerant effect. Such early acceleration can be explained by the chemical and physical effects of GGBS particles. The accelerated cement hydration could be caused by the increased nucleation sites stemming from the ultrafine particles [55]. These particles promote the reaction of cement by means of heterogeneous nucleation, thanks to their high fineness [59]. It was also found that the cumulative heat per gram of binder increases with an increase in slag fineness. The high fineness of SL2 results in an improvement of packing density, thus accelerating the cement reaction. Therefore, the alkalis, as supplied by the cement, and subsequently the Portlandite increased the pozzolanic reaction of SF and BFS [60]. The greater the Portlandite amount, the more enhanced the pozzolanic reaction of BFS, which jointly provides further released heat. These results serve to highlight a double effect of slag addition: a dilution effect and a nucleation site effect. To eliminate the effect of SP, heat flow was measured for some UHPC mixtures at various SP contents. **Figure 8** presents the heat flow evolution of both the Ref_{SF} and SL2-30_{SF} mixtures.

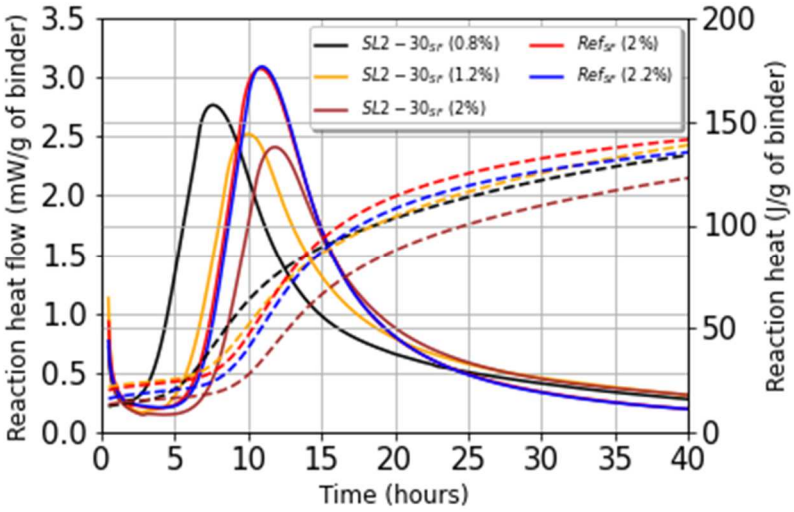

Figure 8 : *Hydration curves of Ref_{SF} and SL2-30_{SF} mixtures at different SP contents.*

As clearly observed, a slight variation in SP content (from 2% to 2.2%) has no effect on the evolution of heat flow of the Ref_{SF} mixture. For SL2-30_{SF} concrete, the increased SP dosage leads to a delay in hydration. For an SP dosage of 1.2%, the time to reach the maximum reaction heat flow is 600 min,

which is 145 min after that of SL2-30_{SF} (0.8%) and 109 min before that of SL2-30_{SF} (2%). Therefore, at a high SP content, the retardation effect cannot be attributed to the slag but rather to the high SP content; the retardation effect of SP may dominate that of slag. Consequently, it is difficult to control the influence of GGBS on UHPC hydration produced with high SP amounts, especially when the SP dosage exceeds the saturation point. Regarding the heat of hydration, it is clear that except for the SL2-30_{SF} (2%) mixture, the other concretes exhibit quite similar heat release values, which implies that increasing the SP dosage from 0.8% to 2% leads to a reduction in heat release.

3.3. Setting time

The initial and final setting times of the UHPC systems are summarized in **Table 4**. As previously stated, these concretes have been prepared with different SP proportions in order to obtain similar workability, and the measurements were mainly performed to understand in detail the effect of slag content and fineness on setting time. Early-age properties are a major technical challenge in the application of blended cementitious materials. As discussed, it is clear that the variation of setting time is basically dependent on the content and fineness of GGBS, as well as on the dosage of SP. Results obtained indicate that SF, SL1 and SL2 have different effects on the UHPC setting times.

Table 4
Vicat setting times of the tested mixtures.

Mixtures	% slag	Initial setting time (min)	Final setting time (min)	Setting time period (min)
Ref_{SF}	0% SL (SF)	345	430	85
SL1-30_{SF}	30% SL1 (SF)	233	375	143
SL1-50_{SF}	50% SL1 (SF)	540	890	350
SL2-30_{SF}	30% SL2 (SF)	80	188	108
SL2-50_{SF}	50% SL2 (SF)	125	360	235
Ref_{SL2}	Reference (SL2)	230	523	293
SL1-30_{SL2}	30% SL1 (SL2)	125	330	205
SL2-30_{SL2}	30% SL2 (SL2)	85	273	188

The addition of SL2, in substitution of SF, results in an acceleration of the initial setting time, which is about 230 min for reference mix Ref_{SL2} vs. 345 min for reference mix Ref_{SF}. The accelerating effect of SL2 is explained by the low dosage of SP in the Ref_{SL2} mixture (2%). The high SP content can cause a strong retardation in setting. Due to the setting retardation effect of SP, the initial setting time of Ref_{SF} reaches 6 h; this outcome is in agreement with previous studies [24,61]. However, it is observed that SF accelerates the final setting time by 53 min compared to Ref_{SL2}. Previous research has revealed that the pozzolanic reaction of SF is fast in comparison with other mineral admixtures. The SF particles act as nucleation sites for the early formation of hydration products [55], which in turn will stimulate cement hydration. The inclusion of SF (Ref_{SF}) reduced the setting time period by 208 min, as compared to reference mixture Ref_{SL2}, thus confirming the higher nucleation effect of SF compared to SL2.

As seen in **Table 4**, the addition of 30% of GGBS as a cement substitution also influences UHPC setting times. It is clear that the presence of low levels of slag accelerates setting times. For instance, for SL1-30_{SF}, the initial and final setting times are accelerated by 1.48 and 1.15 times respectively, in comparison with those of the control mixture Ref_{SF}. This same trend is observed for SL2-30_{SF}. Moreover, it was found that both initial and final setting times are dramatically reduced (by 4.3 and 2.3 times respectively), compared to those of reference concrete Ref_{SF}. These results also indicate that both SL1 and SL2 accelerate the initial and final setting times for mixtures incorporating SL2 in a total substitution of SF (SL1-30_{SL2} and SL2-30_{SL2}), compared to Ref_{SL2}. The acceleration of setting time is more clearly observed in mixtures containing 30% of SL2. The results obtained herein confirm those of the calorimetry tests. As previously mentioned, the surfaces of GGBS particles will act as nucleation sites

for the early reaction products, specifically for the formation of calcium hydroxide, which in turn will stimulate the cement hydration process and offset the dilution effect [47]. Therefore, concretes with a low slag content exhibit shorter setting times than the control mixture. These results agree with those of Yalçınkaya and Yazıcı [35], who confirmed that the remarkable reductions in the initial and final setting times could be attributed to a decrease in the superplasticizer demand and the higher Blaine fineness of GGBS compared to that of the cement particles.

The influence of slag is more sensitive at a 50% replacement rate. For SL1-50_{SF}, SP content equals 2.4%, i.e. 9% higher than that of Ref_{SF}. The initial setting time, final setting time and setting time period are increased respectively by 1.56, 2.07 and 4.11 times, as compared to those of Ref_{SF}. This delay is attributed to the high SP content; SP is largely involved in the simultaneous deceleration of initial and final setting times. With the presence of a high SL1 amount, the dilution effect dominates that of hydration acceleration, which causes longer setting times [11]. The decrease in cement quantity slows the early production of hydrates within the mixture and delays the setting and hardening of the cementitious matrix. It can thus be noted that the phenomenon of dilution governs the hydration and setting process. Indeed, the water-to-cement ratio is 2 times higher in SL1-50_{SF} than in Ref_{SF}. Consequently, 890 min were necessary to reach the final setting, and the setting time period was 350 min for SL1-50_{SF}. This result is in agreement with a previous work conducted by Camiletti *et al.* [55], who indicated that when a high SP content was introduced to achieve a required flowability, the setting time increased relatively. Some works have defined the retardation effect as a delay in hydration, which can be varied depending on: the different adsorption amounts on particles, the concentrations of carboxylic in the aqueous phase, and the charge characteristics of the SP [62]. Conversely, in the case of superfine slag, it was found that 50% of SL2 reduced the initial and final setting times by 2.76 and 1.19 times respectively, in comparison with those of Ref_{SF}. This acceleration is justified by the low SP dosage in SL2-50_{SF} concrete. According to Cyr *et al.* [59], the acceleration effect, due to the presence of fine particles, has not only a chemical origin but a physical one as well. These authors found that the presence of fine particles (with a high specific surface area) could activate cement hydration by means of heterogeneous nucleation. Their results on mineral admixtures reported that the physical effect of fine particles is dominant at an early age, while the pozzolanic effect prevails over the longer term.

Product fineness is an important parameter governing the reaction rate of hydraulic binders. It can be concluded that particle size plays a vital role in affecting the early-age performance of cementitious materials. It was found that an increase in binder fineness leads to an acceleration of both hydration and setting times of the tested UHPC concretes, compared to the same binder with lower fineness. The reactivity of GGBS in a cementitious material depends not only on the chemical components, but also on their fineness [63]. The immediate consequences of rapid hydration are accelerated strength gain and improved durability. It is important to state that increasing the fineness of GGBS can provide a possible solution to reducing the dosage of SP, without affecting the workability of UHPC mixtures and thereby avoiding the hydration delay induced by slag with a lower fineness. The delay in early-age performance development of UHPC containing slag can therefore be compensated by an increase in its fineness, while avoiding any additional chemical and/or thermal activation.

3.4. Chemical shrinkage

According to the literature, the number of investigations conducted on the very early-age shrinkage of UHPC remains very limited. Chemical shrinkage measurements have thus been performed in this study to better clarify the effect of GGBS fineness and content on the early-age shrinkage of UHPC. Chemical shrinkage is a primary mechanism of autogenous shrinkage, hence understanding the role of the individual UHPC components during its early-age chemical shrinkage is critical to controlling the

autogenous shrinkage, which may induce cracking in UHPC structures. The evolution of chemical shrinkage in the various UHPC mixtures is displayed in **Figure 9**.

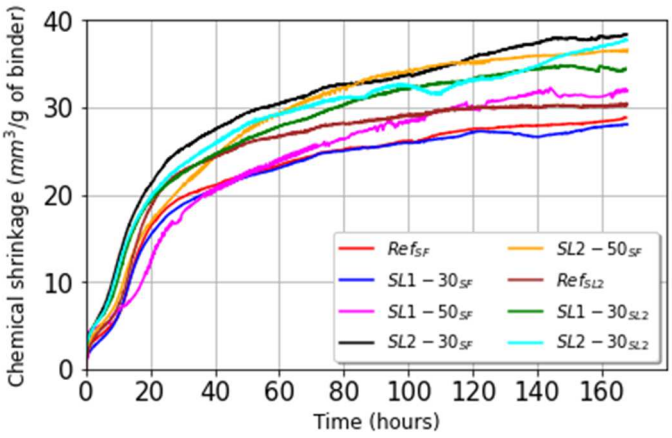

Figure 9 : *Chemical shrinkage of the studied UHPC mixtures.*

As this figure indicates, chemical shrinkage values range from 28 to 38.4 mm^3/g of binder for all mix designs after 168 h. The experimental results can be classified into the following two groups: the first includes SL2-based concretes (SL2-30_{SF}, SL2-50_{SF}, SL1-30_{SL2} and SL2-30_{SL2}), characterized by relatively higher chemical shrinkage than the second group (Ref_{SL2}, Ref_{SF}, SL1-30_{SF} and SL1-50_{SF}).

For the reference concretes (Ref_{SF} and Ref_{SL2}), it is clear that Ref_{SL2} presents a relatively higher chemical shrinkage than Ref_{SF} at all ages. For instance, at 3 days, the chemical shrinkage value of Ref_{SL2} was 27.7 mm^3/g of binder, vs. 24.7 mm^3/g of binder for the Ref_{SF} mix. At 7 days, Ref_{SF} and Ref_{SL2} exhibited a chemical shrinkage of 28.8 and 30.3 mm^3/g of binder, respectively. This result can be explained by the difference in water consumption level of SF and SL2. Because of its extremely high fineness, SF rapidly consumes the water required for hydration. In the Ref_{SL2} mixture, the water content available for the chemical reaction is higher than that of Ref_{SF} due to the low water absorption of SL2 relative to SF (marked by a high specific surface area). This situation leads to an increase in chemical shrinkage. In addition, the mix design is also an important factor that can explain the shrinkage differences. Although a slight difference exists between the two reference mixes, it is important to specify that the results are comparable. This observation confirms the results from the heat of hydration.

The partial substitution of cement by 30% of SL1 caused a slight decrease in the early-age chemical shrinkage. At 24 h, the chemical shrinkage value decreased from 18.1 mm^3/g of binder for Ref_{SF} to 17.0 mm^3/g of binder for the mix incorporating 30% of SL1. Subsequently, as hydration progresses, the difference between Ref_{SF} and SL1-30_{SF} narrows until disappearing completely. At 3 and 7 days, the two mixtures present practically the same chemical shrinkage values. Due to the low SP content of SL1-30_{SF}, the mix reaction was accelerated, resulting in additional shrinkage. Consequently, the chemical shrinkage value of SL1-30_{SF} is close to that of the reference. For a 50% replacement rate, it can be noticed that SL1-50_{SF} shows a less pronounced chemical shrinkage at 24 h (15.4 mm^3/g of binder). Thereafter, the chemical shrinkage of SL1-50_{SF} gradually increases to reach 31.9 mm^3/g of binder at 168 h (vs. 28.8 mm^3/g of binder for Ref_{SF}). All three mixes demonstrated a similar evolution during the first few days. SL1-50_{SF} paste exhibited a higher chemical shrinkage than that of the control mixture. This acceleration resulted in a curve crossing between 72 and 168 h of hydration and could be explained by the beginning of the slag reaction, which produced additional chemical shrinkage. The low chemical shrinkage value at the very early age of SL1-50_{SF} can be attributed to the high SP content, which has a retardation effect.

The chemical shrinkage curve of the mixture containing 30% of SL2 (SL2-30_{SF}) showed a faster evolution. At all ages, SL2-30_{SF} displayed the highest value, as explained by the lower SP content and the high fineness of superfine particles and thus by the accelerated reaction of SL2, which generates an increase in chemical shrinkage. This acceleration is reflected by a crossing of the curve. It is worth mentioning that the mechanical activation promotes the hydration reaction. As proven by the isothermal calorimetry test, the higher the fineness, the greater the hydration rate. At 7 days, the chemical shrinkage value of SL2-30_{SF} was 38.4 mm^3/g of binder, i.e. about 33% and 37% higher than that of the Ref_{SF} and SL1-30_{SF} mixes, respectively. This outcome proves that the large chemical contraction of 38.4 mm^3/g of binder, obtained for a mixture incorporating a superfine slag, is due to both clinker hydration and a greater quantity of fine slag particles. In the case of a 50% substitution rate for SL2, it can be observed that at 24 h of hydration, the chemical shrinkage of SL2-50_{SF} equals 18.5 mm^3/g of binder vs. 18.1 mm^3/g and 23.3 mm^3/g of binder, respectively, for Ref_{SF} and SL2-30_{SF} pastes. At this early stage, the difference in values between the SL2-50_{SF} and SL2-30_{SF} mixtures can be justified by the high SP content of the SL2-50_{SF} mixture, which can induce a delay in the hydration process. However, as hydration progresses, the retardation effect may be offset by the start of slag reactions, leading to the generation of additional chemical shrinkage. Therefore, the difference between the SL2-50_{SF} mixture and the mixture with 30% SL2 was narrowed. At 168 h, SL2-50_{SF} showed a chemical contraction of 36.6 mm^3/g of binder. These same trends are observed with SL1-30_{SL2} and SL2-30_{SL2}. At 24 h, SL1-30_{SL2} exhibited the same chemical shrinkage value as the reference paste Ref_{SL2}, and SL2-30_{SL2} posted a chemical shrinkage value 3% higher than that of the reference paste. The rate of chemical shrinkage evolution in the pastes with slag subsequently increased.

3.5. Autogenous shrinkage

The majority of studies conducted on the autogenous shrinkage of UHPC have focused on linear measurements [26,32,41]. The objective of this experimental work has therefore been to study the volumetric autogenous shrinkage of self-compacting UHPC, in which part of the cement had been replaced by GGBS with two distinct levels of fineness. The early volumetric deformations are converted into linear deformations. In the following, it should be pointed out that results are expressed in µm/m. The evolution of early-age autogenous shrinkage, as measured from the first few minutes after mixing, is shown in **Figure 10**.

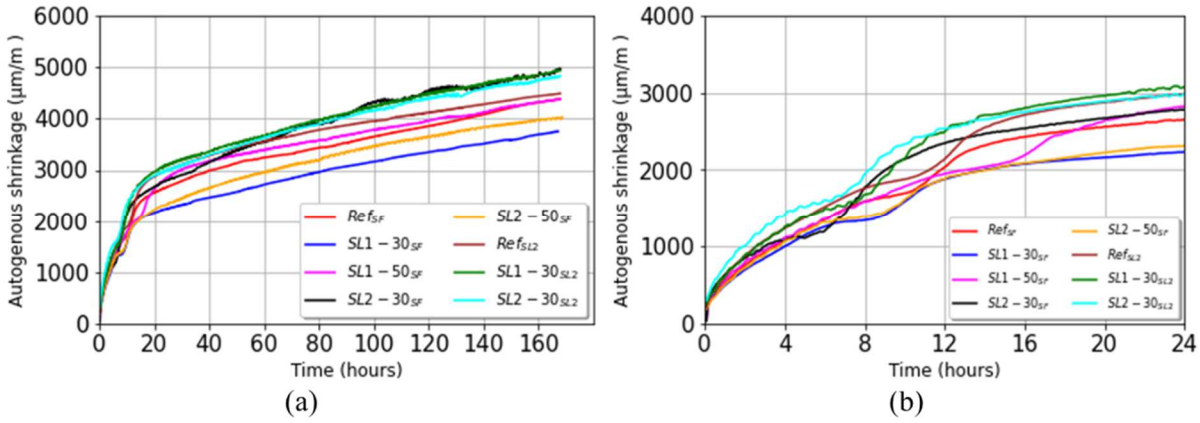

Figure 10 : *Autogenous shrinkage of the studied UHPC mixtures: (a) for the whole study period and (b) for the first 24 hours.*

Figure 10(a) indicates that the various mixtures under investigation exhibit high autogenous shrinkage, with values ranging from 3,753 µm/m (SL1-30_{SF}) to 4,942 µm/m (SL1-30_{SL2}) for all mixtures tested at 7 days. Mounanga *et al.* [41] tested a UHPC with a similar composition (ERPC4) using a horizontal

linear experimental system; they measured an autogenous shrinkage under free conditions of approximately 3,600 µm/m after 100 hours of hydration. These results confirm that autogenous shrinkage is very high during the first few days, i.e. between 24 and 72 h after casting. It is clearly apparent that most of the autogenous shrinkage has occurred within the first few hours after mixing. At 24 h, at least 56% of the total volumetric autogenous shrinkage (measured at 7 d) had been recorded for all mixtures being considered. In focusing on the first 24 hours of hydration, the gap between the autogenous shrinkage curves of the various UHPC mixtures may be due to the varying SP content and/or the presence of mineral additions with different reactivities. As an example, **Figure 10(b)** clearly shows that the appearance of a second inflection point for the SL1-50SF mixture (at about 15 h) is later than that of SL1-30SF (at about 8.5 h). This delay can be explained by the combined dilution / SP content effect. After 24 hours, the autogenous shrinkage curve trends are quite linear and parallel to one another.

For the reference mixtures (Ref_{SF} and Ref_{SL2}), it was found that Ref_{SL2} exhibited slightly higher autogenous shrinkage than Ref_{SF} at all ages, yet keep in mind that the results remain comparable. This trend confirms the results obtained from the chemical shrinkage test. At 168 h, the autogenous deformation value of Ref_{SL2} equaled 4,483 µm/m, vs. 4,380 µm/m for Ref_{SF}. While the vast majority of studies demonstrate that SF increases the autogenous shrinkage of UHPC, though this effect was not observed in our case. A reduction in SF content (9% in this paper) would form a coarser pore structure and thereby reduce autogenous shrinkage. A second cause of the higher deformation of the SL2-blended matrix (Ref_{SL2}) would be the large SL2 content due to the volume substitution.

As observed in **Figure 10**, the concrete containing 30% of SL1 (SL1-30_{SF}) features less autogenous shrinkage over the first 7 days. It was found that 30% of SL1 (for the SL1-30_{SF} mixture) decreased autogenous shrinkage by approximately 15.8%, 14.5% and 14.3% at 24 h, 72 h and 168 h, respectively, vs. reference mix Ref_{SF}. These findings corroborate the results of a previous study [64], whose authors reported that the total shrinkage of UHPC incorporating steel slag powder (SSP) is less than that of UHPC without SSP. As the amount of SL1 increases, water consumption also increases; thus, the self-desiccation of UHPC becomes more pronounced. It is important to note that SL1-50_{SF} induces a slight increase in autogenous shrinkage. For example, the autogenous shrinkage increased by 4.6% at 3 days compared to Ref_{SF}. The delay in hydration caused by SP (the SP content in SL1-50_{SF} is greater than in Ref_{SF} and SL1-30_{SF}), and the latent SL1 reaction resulted in both a setting retardation and an extension of the deformation phase dominated by chemical shrinkage, and consequently autogenous shrinkage.

The addition of 30% high fineness slag (SL2) increases autogenous shrinkage because superfine slag increases the self-desiccation by consuming the pore solution (calcium hydroxide) in a small capillary pore structure [65]. Compared to Ref_{SF}, an increase of 12.8% was recorded for the SL2-30_{SF} mixture at 7 days. This increased effect can be explained by the high reactivity of SL2. As slag fineness increases, the hydration of cementitious materials increases at an early age; moreover, water consumption increases, hence the UHPC self-desiccation becomes more severe. In contrast with a substitution rate of 30%, it is clear that SL2-50_{SF} has a lower autogenous shrinkage than Ref_{SF} and SL2-30_{SF}; this phenomenon is related to the dilution effect. Another explanation for the lower autogenous deformation of SL2-50_{SF} involves the interparticle forces. At a high replacement level, attractive forces may dominate, and the superfine slag particles may behave like coarse slag. For this reason, the SL2-50_{SF} mixture exhibits a shrinkage response quite similar to that of SL1-30_{SF}. The results obtained agree with those of Yang *et al.* [66], who concluded that as the cement replacement percentage with phosphorous slag (PS) increases, hydration can be slowed and the cement dilution effect can improve UHPC volume stability. In other words, a large volume of PS can decrease the autogenous shrinkage of UHPC.

Similar to SL2-30_{SF}, both SL1-30_{SL2} and SL2-30_{SL2} are more susceptible to self-desiccation and, consequently, to autogenous shrinkage. These concretes display a behavior close to that of SL2-30_{SF}, as

illustrated in **Figure 10**. The samples containing 30% of slag (SL1 or SL2), with SL2 in replacement of SF, exhibited a significant amount of autogenous shrinkage at an early age. In fact, the incorporation of SL2 can accelerate the hydration process of the (C_3S) clinker phase due to the extensive and highly reactive surface of particles, resulting in the formation of more calcium silicate hydrate (C-S-H) at an early age. The physical effect of GGBS particles, via the heterogeneous nucleation of hydrates produced, leads to an accelerated hydration process. The increase in Portlandite content yields greater pozzolanic activity of the superfine slag. The pozzolanic reaction of GGBS increases the consumption of calcium hydroxide, which in turn increases water consumption by means of both hydraulic and pozzolanic reactions, thus inducing more self-desiccation. Therefore, GGBS increases the autogenous shrinkage due to the refined pore structure and moreover increases water depletion [37]. The slag additive is known to have a lower Young's modulus, which induces more severe shrinkage than a cement paste submitted to an identical internal capillary tension. Lura *et al.* [27] reported that the finer pore distribution of slag-cement pastes increased capillary depression, thus engendering a more pronounced shrinkage.

3.6. Cross analysis

The experimental work herein suggests that incorporating 30% slag (SL1 or SL2) reduces the SP dosage, yet without affecting workability. Isothermal calorimetry results have shown that the presence of a low slag content (30%) serves to accelerate the hydration process. This acceleration effect, due to the presence of fine particles, is both of chemical and physical origin. It should be noted that the reduced SP content is also involved in the acceleration of hydration. The increased hydration rate leads to a reduction in setting time. With the high SL1 content (50%), it was found that the dilution effect dominates and slag particles increase the SP demand, resulting in delayed hydration and increased setting time. For 50% of superfine slag, an acceleration effect was observed. Due to the smooth surface and the physical effect of SL2 particles, the SP demand has decreased.

Since chemical shrinkage is a direct consequence of the hydration reactions, the accelerated cement hydration due to the presence of superfine slag induces an increase in the chemical shrinkage rate. In addition, the presence of GGBS modifies hydration products. Due to its relatively high reactivity, SL2 can react more rapidly than SL1. In order to relate Le Chatelier's contraction to the physicochemical evolution of the material, the results of chemical shrinkage as a function of the heat of hydration are presented in **Figure 11**. It can be clearly seen that for each UHPC mix, a quasi-linear relationship exists between the two parameters, regardless of GGBS dosage and fineness. This result indicates that the slag effect on UHPC chemical shrinkage can mainly be considered as a kinetic effect at the early age.

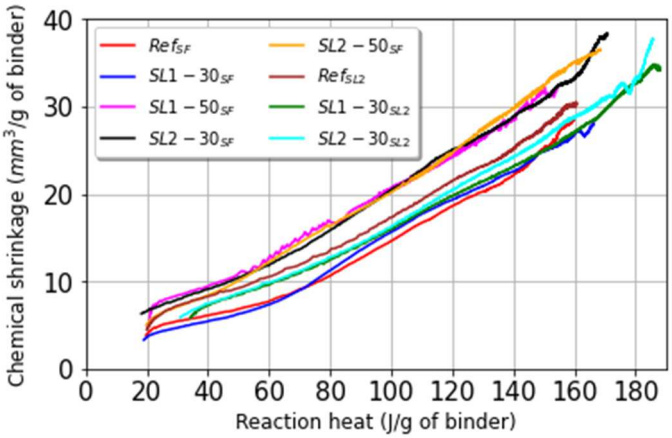

Figure 11 : *Chemical shrinkage vs. hydration heat of UHPC mixtures.*

This section will present the results of the chemical and autogenous shrinkage kinetics, as well as those of hydration kinetics, in order to draw a comparative analysis of the various deformations corresponding to the evolution of material heat flow. **Figure 12** illustrates these different parameters for the reference concrete (Ref_{SF}). The free chemical shrinkage and autogenous shrinkage are given in mm^3/g of binder. The hydration heat flow is expressed in mW/g of binder.

It can be seen that the hydration heat flow reaches its maximum at 657 min. At approximately the same time, the chemical and autogenous shrinkage curves transit from one regime to another, passing through an inflection point. The thermal peak reached reflects the high chemical activity of the cement. The transition between chemical shrinkage and self-desiccation is generally marked by a flattening of the autogenous shrinkage curve. Up to the final setting time, the chemical shrinkage and autogenous shrinkage are nearly equal. After the final set, a considerable difference is observed between these values (with 17.3 mm^3/g of binder for Ref_{SF} at 7 days). The point marking the transition between these two deformations generally indicates the formation of the solid skeleton, i.e. the setting period, during which the material begins to harden and develop a stiffness that allows it to resist deformation. For the Ref_{SF} mixture, the initial and final setting times equal 345 and 430 min, respectively. It can be concluded that for the reference sample, the divergence in chemical and autogenous shrinkage occurs during the setting period.

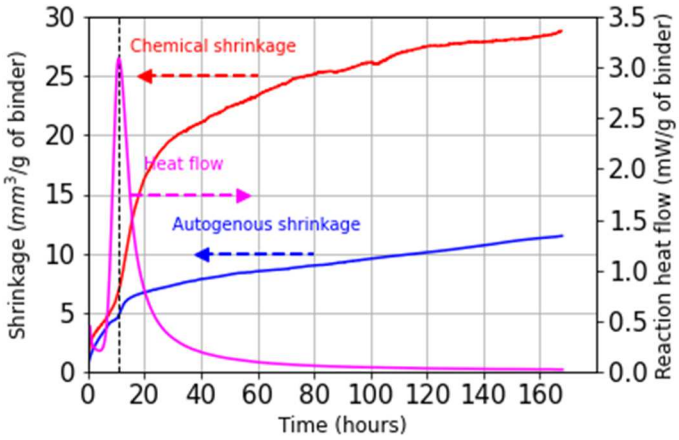

Figure 12 : *Deformation and hydration heat flow kinetics of* Ref_{SF}.

Autogenous shrinkage is particularly problematic at the very early age in cementitious matrices with low w/b ratios; it may even be a cause of early material cracking. The high binder content considerably increases its amplitude at an early age and induces a high risk of early cracking. To identify the actual effect of autogenous shrinkage on the cracking risk of GGBS-based UHPC, it is important to investigate in depth the evolution of this deformation. It is interesting to point out that the reported evolution in the autogenous deformation under free conditions depends largely on the choice of "time-zero" (the time for the beginning of autogenous shrinkage measurement) [67]. An incorrect definition of this reference time can lead to various interpretations of the behavior of the same concrete [68]. In this section, the initial setting time was considered as the time corresponding to the start of the deformation measurement. The results of chemical shrinkage and volumetric autogenous shrinkage, both monitored from the initial setting time, are given in **Figures 13** and **14**, respectively.

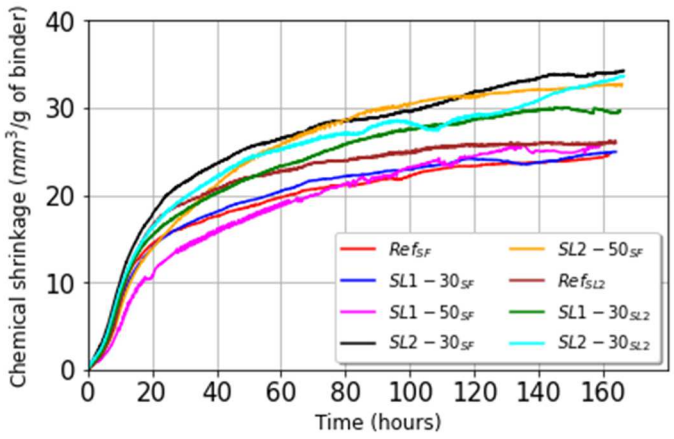

Figure 13 : *Chemical shrinkage of the UHPC mixtures with the "time-zero" (the inial setting time).*

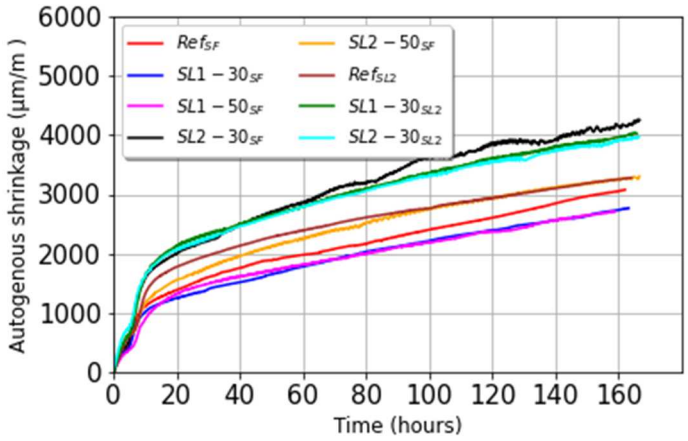

Figure 14 : *Autogenous shrinkage of the UHPC mixtures with the "time-zero" (the inial setting time).*

As clearly seen in **Figure 13**, the evolution of the chemical contraction measured from the initial setting time follows the same trend as chemical shrinkage curves recorded in the fresh state (i.e. immediately after the end of mixing). It is well known that Le Chatelier's contraction develops before the setting of the matrix; it primarily corresponds to the dissolution of clinker minerals, the hydration of anhydrite and the precipitation of ettringite [69], as well as to the negative balance between the absolute volume of hydrates formed and that of the reactants. The observed reduction in amplitudes is explained by the fact that a portion of chemical shrinkage developed before the setting. **Figure 14** shows that a significant portion (more than 47%) of the autogenous shrinkage (as calculated from the initial setting time) of all mixes studied during the first 7 days occurred within the first 24 hours after the initial setting time. More than 14% of the autogenous shrinkage (as monitored from the first few minutes after mixing) was achieved before the initial setting time. The trend for the autogenous shrinkage curves of UHPC mixtures with "time zero" (the initial setting time) was slightly changed. These changes are correlated with the change in microstructure around the initial setting time. After "time zero", the rigid skeleton was created with sufficient rigidity, and the chemical shrinkage could not be fully transformed into an external volume change [67]. It was found that SL1-30_{SF} and SL1-50_{SF} exhibited the same autogenous strain, which is lower than that of Ref_{SF}. The autogenous deformation of these concretes, expressed from this time zero, is characterized by an expansion of their cement matrix. These observations are in agreement with those of Darquennes *et al.* [68]. The three mixtures (SL2-30_{SF}, SL1-30_{SL2} and SL2-30_{SL2}) always present the highest risk of cracking. It is obvious that the autogenous shrinkage of these mixes increases faster than for the reference concretes, with the advancement of the hydration reaction. The finest pore

size is slightly larger for SL2. For this reason, the pronounced autogenous shrinkage is observed for SL2-30_{SF}, SL1-30_{SL2} and SL2-30_{SL2} blends. The main mechanism driving self-desiccation is the variation of capillary depression. Based on the Laplace and Kelvin Laws, the intensity of capillary depression is inversely proportional to pore radius. As the hydration reaction progresses, the generation of supplementary C-S-H by slag hydration fills the porosity developed at an early age. Therefore, at a high SL2 replacement (SL2-50_{SF}), a reduction in autogenous shrinkage was recorded, as compared to SL2-30_{SF}.

It can be concluded that increasing slag fineness increases autogenous shrinkage and, consequently, the risk of cracking. This phenomenon is related to the finer porosity, which leads to a greater capillary depression. One possible explanation for the difference in shrinkage behavior between ordinary slag and superfine slag might pertain to the internal relative humidity. As mentioned above, SL2 is characterized by a high reactivity. The pozzolanic reaction of SL2 increases the consumption of calcium hydroxide, which in turn increases water consumption. This higher water consumption then lowers the internal relative humidity, hence a greater amount of self-desiccation.

4. Conclusions

The present paper is aimed at developing more sustainable UHPC, in favor of an efficient GGBS application. The experimental work herein has focused on characterizing the effects of incorporating GGBS on: workability, early-age hydration, setting time, chemical and volumetric autogenous shrinkage of multi-component UHPC containing Portland cement, and reactive mineral additions (SF and GGBS). From an analysis of the results obtained, the following conclusions can be drawn:

- The replacement of 30% of cement by GGBS decreased the SP content in UHPC mixtures. At 30% replacement level, GGBS improves density packing, enhances workability, accelerates setting times, and promotes the cement hydration process through the nucleation site effect.

- The partial replacement of OPC by 50% of ordinary slag caused an increase in the amount of SP required for the desired flowability. In this case, the lubrication effect of SL1 and the fluidizing effect of SP seem to be attenuated by the water demand of slag particles. This phenomenon delays cement hydration and prolongs setting times. In the case of a high ordinary slag level, the dilution effect is dominant.

- The use of slag with high fineness significantly improves the workability of UHPC mixtures (through a lower SP dosage for the same workability). The beneficial filling effect of the superfine slag tends to accelerate both setting times and cement hydration. These effects are noticeable even for a cement substitution rate with 50% of finer GGBS. These findings are mainly attributed to both the dilution and heterogeneous nucleation effects.

- The substitution of 30% of cement by low fineness slag caused a slight decrease in early-age chemical and autogenous shrinkage, due to its lower reactivity. The most pronounced shrinkage was observed, more clearly, in the mixtures containing 30% of superfine slag. The higher autogenous shrinkage of superfine slag-blended mixtures can be explained by higher slag fineness, higher chemical shrinkage and a lower Young's modulus of the slag-cement matrix. Another reason for the large deformation of the blended matrix would be the finer pore distribution of slag-cement matrices, which increases the capillary depression, thus leading to more pronounced shrinkage and, consequently, a high risk of cracking.

- A high substitution rate (50%) is not considered to have any significant effect on chemical contraction, compared to 30%. However, this replacement level significantly modifies the evolution of autogenous shrinkage.

In conclusion, a more eco-friendly UHPC has been designed and optimized. High replacement rates of GGBS, extending up to 50%, have been used to reduce the cement content in UHPC. Increasing slag fineness is one of the successful paths to improving reactivity, thus accelerating the hydration process, which can enhance early strength development. Superfine slag has proven to be effective in completely replacing silica fume in the manufacture of UHPC. To the best of our knowledge, this effort marks the first time such an innovative approach has been employed. Superfine slag was found to increase shrinkage, and thus the cracking risk, which does require special attention. Due to the scarcity of data on this fundamental issue, the question of optimal fineness, in meeting the various technical, economic and environmental requirements, remains an open one. Therefore, further research is necessary to ensure a proper control of this kind of mechanical activation. Knowledge of the optimal fineness, which is a key parameter, will enable better quantifying the effectiveness of GGBS regarding the properties of multi-component UHPC.

Acknowledgments

The financial support provided by the University of Tunis El Manar (Tunisia) and ECOCEM Materials is greatly appreciated. The authors would also like to express their sincere gratitude for the technical assistance in mixture manufacturing and characterization offered by Jérôme Carriat, Véronique Queyrat and Florencio Tharladiere.

References

[1] E. Ghafari, M. Arezoumandi, H. Costa, E. Júlio, Influence of nano-silica addition in the durability of UHPC, Constr. Build. Mater. 94 (2015) 181–188, https://doi.org/10.1016/j.conbuildmat.2015.07.009.

[2] J. Du, W. Meng, K. H. Khayat, Y. Bao, P. Guo, Z. Lyu, A. Abu-obeidah, H. Nassif, H. Wang, New development of ultra-high-performance concrete (UHPC), Composites Part B 224 (2021) 109220, https://doi.org/10.1016/j.compositesb.2021.109220.

[3] UNSTATS, Greenhouse gas emissions by sector (absolute values), United Nation Statistical Division, Springer, 2010.

[4] R. Yu, P. Spiesz, H.J.H. Brouwers, Mix design and properties assessment of Ultra-High Performance Fibre Reinforced Concrete (UHPFRC), Cem. Concr. Res. 56 (2014) 29–39, https://doi.org/10.1016/j.cemconres.2013.11.002.

[5] E. Denarié, E. Brühwiler, Strain Hardening Ultra-high Performance Fibre Reinforced Concrete: Deformability versus Strength Optimization, Int. J. Restauration Build. Monuments 17 (6) (2011) 397–410 (Aedificatio), https://doi.org/10.1515/rbm-2011-6480.

[6] G. Habert, E. Denarié, A. Šajna, P. Rossi, Lowering the global warming impact of bridge rehabilitations by using Ultra High Performance Fibre Reinforced Concretes, Cem. Concr. Comput. 38 (2013) 1–11, https://doi.org/10.1016/j.cemconcomp.2012.11.008.

[7] T. Ahmed, M. Elchalakani, A. Karrech, M.S. Mohamed Ali, L. Guo, Development of ECO-UHPC with very-low-C3A cement and ground granulated blast-furnace slag, Constr. Build. Mater. 284 (2021) 122787, https://doi.org/10.1016/j.conbuildmat.2021.122787.

[8] R. Yu, P. Spiesz, H.J.H. Brouwers, Development of an eco-friendly Ultra-High Performance Concrete (UHPC) with efficient cement and mineral admixtures uses, Cem. Concr. Compos. 55 (2015) 383–394, https://doi.org/10.1016/j.cemconcomp.2014.09.024.

[9] N. V. Tuan, G. Ye, K. Van Breugel, A.L.A. Fraaij, D.D. Bui, The study of using rice husk ash to produce ultra high performance concrete, Constr. Build. Mater. 25 (2011) 2030–2035, https://doi.org/10.1016/j.conbuildmat.2010.11.046.

[10] H. Yazıcı, M.Y. Yardımcı, H. Yig˘iter, S. Aydın, S. Türkel, Mechanical properties of reactive powder concrete containing high volumes of ground granulated blast furnace slag, Cem. Concr. Compos. 32 (2010) 639–648, https://doi.org/10.1016/j.cemconcomp.2010.07.005.

[11] O.M. Abdulkareem, A.Ben Fraj, M. Bouasker, A. Khelidj, Mixture design and early age investigations of more sustainable UHPC, Constr. Build. Mater. 163 (2018) 235–246, https://doi.org/10.1016/j.conbuildmat.2017.12.107.

[12] O.M. Abdulkareem, A.Ben Fraj, M. Bouasker, A. Khelidj, Effect of chemical and thermal activation on the microstructural and mechanical properties of more sustainable UHPC, Constr. Build. Mater. 169 (2018) 567–577, https://doi.org/10.1016/j.conbuildmat.2018.02.214.

[13] S. B. Duraman, Ian G. Richardson, Microstructure & properties of steel-reinforced concrete incorporating Portland cement and ground granulated blast furnace slag hydrated at 20 °C, Cem. Concr. Res. 137 (2020) 106193, https://doi.org/10.1016/j.cemconres.2020.106193.

[14] Ç. Yalçınkaya, O. Çopuro˘glu, Hydration heat, strength and microstructure characteristics of UHPC containing blast furnace slag, Journal of Building Engineering 34 (2021) 101915, https://doi.org/10.1016/j.jobe.2020.101915.

[15] O.M. Abdulkareem, A.Ben Fraj, M. Bouasker, L. Khouchaf, A. Khelidj, Microstructural investigation of slag-blended UHPC: The effects of slag content and chemical/thermal activation, Constr. Build. Mater. 292 (2021) 123455, https://doi.org/10.1016/j.conbuildmat.2021.123455.

[16] N. S. Ha, S. S. Marundrury, T. M. Pham, E. Pournasiri, F. Shi, H. Hao, Effect of grounded blast furnace slag and rice husk ash on performance of ultra-high-performance concrete (UHPC) subjected to impact loading, Constr. Build. Mater. 329 (2022) 127213, https://doi.org/10.1016/j.conbuildmat.2022.127213.

[17] S. Gupta, Effect of content and fineness of slag as high volume cement replacement on strength and durability of ultra-high performance mortar, J. Build. Mater. Struct. 3 (2016) 43–54, https://doi.org/10.34118/jbms.v3i2.23.

[18] D.P. Bentz, A review of early-age properties of cement-based materials, Cem. Concr. Res. 38 (2008) 196–204, https://doi.org/10.1016/j.cemconres.2007.09.005.

[19] D.Y. Yoo, S. Kim, M.J. Kim, Comparative shrinkage behavior of ultra-high-performance fiberreinforced concrete under ambient and heat curing conditions, Constr. Build. Mater. 162 (2018) 406–419, https://doi.org/10.1016/j.conbuildmat.2017.12.029.

[20] S. Pyo, H.-K. Kim, Fresh and hardened properties of ultra-high performance concrete incorporating coal bottom ash and slag powder, Constr. Build. Mater. 131 (2017) 459–466, https://doi.org/10.1016/j.conbuildmat.2016.10.109.

[21] B. Luzu, R. Trauchessec, A. Lecomte, Packing density of limestone calcined clay binder, Powder Technology 408 (2022) 117702, https://doi.org/10.1016/j.powtec.2022.117702.

[22] A. Korpa, T. Kowald, R. Trettin, Hydration behaviour, structure and morphology of hydration phases in advanced cement-based systems containing micro and nanoscale pozzolanic additives, Cem. Concr. Res. 38 (2008) 955–962, https://doi.org/10.1016/j.cemconres.2008.02.010.

[23] H. Kim, T. Koh, S. Pyo, Enhancing flowability and sustainability of ultra high performance concrete incorporating high replacement levels of industrial slags, Constr. Build. Mater. 123 (2016) 153–160, https://doi.org/10.1016/j.conbuildmat.2016.06.134.

[24] P. Richard, M. Cheyrezy, Composition of reactive powder concretes, Cem. Concr. Res. 25 (7) (1995) 1501–1511, https://doi.org/10.1016/0008-8846(95)00144-2.

[25] M.C.G. Juenger, R. Siddique, Recent advances in understanding the role of supplementary cementitious materials in concrete, Cem. Concr. Res. 78 (2015) 71–80, https://doi.org/10.1016/j.cemconres.2015.03.018.

[26] P. Shen, L. Lu, Y. He, M. Rao, Z. Fu, F. Wang, S. Hu, Experimental investigation on the autogenous shrinkage of steam cured ultra-high performance concrete, Constr. Build. Mater. 162 (2018) 512–522, https://doi.org/10.1016/j.conbuildmat.2017.11.172.

[27] P. Lura, O.M. Jensen, J. Weiss, Cracking in cement paste induced by autogenous shrinkage, Mater. Struct. 42 (8) (2009) 1089–1099, https://doi.org/10.1617/s11527-008-9445-z.

[28] D.-Y. Yoo, J.-J. Park, S.-W. Kim, Y.-S. Yoon, Early age setting, shrinkage and tensile characteristics of ultra high performance fiber reinforced concrete, Constr. Build. Mater. 41 (2013) 427–438, https://doi.org/10.1016/j.conbuildmat.2012.12.015.

[29] P.P. Li, Q.L. Yu, H.J.H. Brouwers, Effect of PCE-type superplasticizer on early-age behaviour of ultra-high performance concrete (UHPC), Constr. Build. Mater. 153 (2017) 740–750, https://doi.org/10.1016/j.conbuildmat.2017.07.145.

[30] A. ZENATI, M. TAHLAITI, A. KHELIDJ, M.N. OUDJIT, Hydration, Shrinkages and Mechanical Properties of Ultra High Performance Concrete Containing Blast Furnace Slag and Algerian Dune Sand, International Journal of Engineering Research in Africa, 42 (2019) 86-99, https://doi.org/10.4028/www.scientific.net/JERA.42.86.

[31] E. Erten, Ç. Yalçinkaya, A. Beglarigale, H. Yiğiter, H. YazicI, Erken yaş büzülme çatlaklarının lif içeren/içermeyen ultra yüksek performanslı betona gömülü donatı korozyonuna etkisi. Gazi Üniversitesi Mühendislik Mimar. Fakültesi Derg. 32 (2017) 1347–1364, https://doi.org/10.17341/gazimmfd.369857.

[32] L. Caixia, S. Zhilin, Y. Liqi, Z. Guorong, Study on autogenous shrinkage characteristic and mechanism of ultra-high performance cementitous composite. IOP Conf. Ser.: Mater. Sci. Eng. 324, 012037, 2018, 10.1088/1757-899X/324/1/012037.

[33] L. Yang, C. Shi, Z. Wu, Mitigation techniques for autogenous shrinkage of ultra-high-performance concrete – A review, Composites Part B 178 (2019) 107456, https://doi.org/10.1016/j.compositesb.2019.107456.

[34] S. Park, S. Wu, Z. Liu, S. Pyo, The Role of Supplementary Cementitious Materials (SCMs) in Ultra High Performance Concrete (UHPC): A Review, Materials 14 (2021) 1406–1472, https://doi.org/10.3390/ma14061472.

[35] Ç. Yalçınkaya, H. Yazıcı, Effects of ambient temperature and relative humidity on early-age shrinkage of UHPC with high-volume mineral admixtures, Constr. Build. Mater. 144 (2017) 252–259, https://doi.org/10.1016/j.conbuildmat.2017.03.198.

[36] E. Ghafari, S.A. Ghahari, H. Costa, E. Júlio, A. Portugal, L. Durães, Effect of supplementary cementitious materials on autogenous shrinkage of ultra-high performance concrete, Constr. Build. Mater. 127 (2016) 43–48, https://doi.org/10.1016/j.conbuildmat.2016.09.123.

[37] Z. Liu, S. El-Tawil, W. Hansen, F. Wang, Effect of slag cement on the properties of ultra-high performance concrete. Constr. Build. Mater. 190 (2018) 830–837, https://doi.org/10.1016/j.conbuildmat.2018.09.173.

[38] E. Tazawa, S. Miyazawa, Influence of cement and admixture on autogenous shrinkage of cement paste, Cem. Concr. Res. 25 (1995) 281–287, https://doi.org/10.1016/0008-8846(95)00010-0.

[39] K.M. Lee, H.K. Lee, S.H. Lee, G.Y. Kim, Autogenous shrinkage of concrete containing granulated blast-furnace slag, Cem. Concr. Res. 36 (2006) 1279–1285, https://doi.org/10.1016/j.cemconres.2006.01.005.

[40] P. Lura, K. van Breugel, I. Maruyama, Effect of curing temperature and type of cement on early-age shrinkage of high-performance concrete, Cem. Concr. Res. 31 (2001) 1867–1872, https://doi.org/10.1016/S0008-8846(01)00601-9.

[41] P. Mounanga, K. Cherkaoui, A. Khelidj, M. Courtial, M.-N. de Noirfontaine, F. Dunstetter, Extrudable reactive powder concretes hydration, shrinkage and transfer properties, Eur. J. Environ. Civ. Eng. 16 (2012) 99–114, https://hal.archives-ouvertes.fr/hal-00719593.

[42] A. Wetzel, C. Glotzbach, K. Maryamh, B. Middendorf, Microstructural investigations on the skinning of ultra-high performance concrete, Cem. Concr. Compos. 57 (2015) 27-33, https://doi.org/10.1016/j.cemconcomp.2014.11.010.

[43] Ç. Yalçınkaya, O. Çopurog˘lu, Elephant skin formation on UHPC surface: Effects of climatic condition and blast furnace slag content, Constr. Build. Mater. 268 (2021) 121126, https://doi.org/10.1016/j.conbuildmat.2020.121126.

[44] EN 12350-8: testing fresh concrete – Part 8: self-compacting concrete – Slump-flow test, 2019, European Standard.

[45] EN 196-3, AFNOR, Methods of Testing Cement - Part 3: Determination of Setting Times and Soundness, 2017, European standards.

[46] M. Bouasker, P. Mounanga, P. Turcry, A. Loukili, A. Khelidj, Chemical shrinkage of cement pastes and mortars at very early age: effect of limestone filler and granular inclusions. Cem. Concr. Compos. 30(1) (2008) 13–22, https://doi.org/10.1016/j.cemconcomp.2007.06.004.

[47] P. Mounanga, M.I.A. Khokhar, R. El Hachem, A. Loukili, Improvement of the early-age reactivity of fly ash and blast furnace slag cementitious systems using limestone filler, Mater. Struct. 44 (2011) 437–453, https://doi.org/10.1617/s11527-010-9637-1.

[48] M. Bouasker, F. Grondin, P. Mounanga, A. Pertué, A. Khelidj, Improved measurement methods for autogenous shrinkage of cement mortars at very early age, 2nd International Symposium on Advances in Concrete through Science and Engineering 11-13 September 2006, Quebec City, Canada.

[49] F. Lavergne, R. Belhadi, J. Carriat, A. Ben Fraj, Effect of nano-silica particles on the hydration, the rheology and the strength development of a blended cement paste, Cem. Concr. Compos. 95 (2019) 42–55, https://doi.org/10.1016/j.cemconcomp.2018.10.007.

[50] B. Samet, M. Chaabouni, Characterization of the Tunisian blast-furnace slag and its application in the formulation of a cement, Cem. Concr. Res. 34 (2004) 1153–1159, https://doi.org/10.1016/j.cemconres.2003.12.021.

[51] H. Kim, T. Koh, S. Pyo, Enhancing flowability and sustainability of ultra high performance concrete incorporating high replacement levels of industrial slags, Constr. Build. Mater. 123 (2015) 153–160, https://doi.org/10.1016/j.conbuildmat.2016.06.134.

[52] F. de Larrard, Structures granulaires et formulation des bétons - Concrete Mixture - Proportionning - A scientific approach, Modern technology Series, E & FN SPON, Londres, 1999.

[53] A. Korpa, R. Trettin, Ultra high performance cement-based composites with advanced properties containing nanoscale pozzolans, in: Proceedings of the Second International Symposium on Ultra High Performance Concrete, Kassel, Germany, 2008.

[54] J. Zelić, D. Rušić, D. Veža, R. Krstulović, The role of silica fume in the kinetics and mechanisms during the early stage of cement hydration, Cem. Concr. Res. 30 (2000), 1655–1662, https://doi.org/10.1016/S0008-8846(00)00374-4.

[55] J. Camiletti, A. M. Soliman, and M. L. Nehdi, Effects of nano-and micro-limestone addition on early-age properties of ultrahigh-performance concrete, Mater. Struct., 46 (6) (2013) 881–898, https://doi.org/10.1617/s11527-012-9940-0.

[56] J. Xi, J. Liu, K. Yang, S. Zhang, F. Han, J. Sha, X. Zheng, Role of silica fume on hydration and strength development of ultra-high performance concrete, Constr. Build. Mater. 338 (2022) 127600, https://doi.org/10.1016/j.conbuildmat.2022.127600.

[57] F. Han, Z. Zhang, D. Wang, P. Yan, Hydration kinetics of composite binder containing slag at different temperatures, J Therm Anal Calorim 121 (2015) 815–827, https://doi.org/10.1007/s10973-015-4631-z.

[58] Y. Li, C. Yang, Y. Zhang, J. Zheng, H. Guo, M. Lu, Study on dispersion, adsorption and flow retaining behaviors of cement mortars with TPEG-type polyether kind polycarboxylate superplasticizers, Constr. Build. Mater. 64 (2014) 324– 332, https://doi.org/10.1016/j.conbuildmat.2014.04.050.

[59] M. Cyr, P. Lawrence, E. Ringot, Mineral admixtures in mortars. Quantification of the physical effects of inert materials on short-term hydration, Cem. Concr. Res. 35 (2005) 719–730, https://doi.org/10.1016/j.cemconres.2004.05.030.

[60] T. Merzouki, M. Bouasker, N. Khalifa, P. Mounanga, Contribution to the modeling of hydration and chemical shrinkage of slag-blended cement at early age. Constr. Build. Mater. 44 (2013) 368-380, https://doi.org/10.1016/j.conbuildmat.2013.02.022.

[61] S. Abbas, M.L. Nehdi, M.A. Saleem, Ultra-high performance concrete: mechanical performance, durability, sustainability and implementation challenges, Int. J. Concr. Struct. Mater. 10 (3) (2016) 271–295, https://doi.org/10.1007/s40069-016-0157-4.

[62] Y. Zhang, X. Kong, Correlations of the dispersing capability of NSF and PCE types of superplasticizer and their impacts on cement hydration with the adsorption in fresh cement pastes, Cem. Concr. Res. 69 (2015) 1–9, https://doi.org/10.1016/j.cemconres.2014.11.009.

[63] S.C. Pal, A.Mukherjee, S.R. Pathak, Investigation of hydraulic activity of ground granulated blast furnace slag in concrete, Cem. Concr. Res. 33 (2003) 1481–1486, https://doi.org/10.1016/S0008-8846(03)00062-0.

[64] S. Li, S. Cheng, L. Mo, M. Deng, Effects of steel slag powder and expansive agent on the properties of ultra-high performance concrete (UHPC): Based on a case study. Materials 2020, 13, 683, https://doi.org/10.3390/ma13030683.

[65] Z. Liu, W. Hansen, Aggregate and slag cement effects on autogenous shrinkage in cementitious materials. Constr. Build. Mater. 121 (2016) 429–436, https://doi.org/10.1016/j.conbuildmat.2016.06.012.

923 [66] R. Yang, R. Yu, Z. Shui, X. Gao, X. Xiao, X. Zhang, Y. Wang, Y. He, Low carbon design of an Ultra-High Performance Concrete
924 (UHPC) incorporating phosphorous slag. J. Clean. Prod. 240 (2019) 118157, https://doi.org/10.1016/j.jclepro.2019.118157.

925 [67] H. Huang, G. Ye, Examining the "time-zero" of autogenous shrinkage in high/ultra-high performance cement pastes, Cem. Concr. Res.
926 97 (2017) 107–114, https://doi.org/10.1016/j.cemconres.2017.03.010.

927 [68] A. Darquennes, S. Staquet, M-P. Delplancke-Ogletree, B. Espion, Effect of autogenous deformation on the cracking risk of slag cement
928 concretes, Cem. Concr. Compos. 33 (2011) 368–379, https://doi.org/10.1016/j.cemconcomp.2010.12.003.

929 [69] F. Beltzung, F.H. Wittmann, "Early chemical shrinkage due to dissolution and hydration of cement", Mater. Struct., 34 (5) (2001) 279–
930 283, https://doi.org/10.1007/BF02482207.